A FIBRE BEAM COLUMN ELEMENT FOR MODELLING THE FLEXURE-SHEAR INTERACTION IN THE NON-LINEAR ANALYSIS OF RC STRUCTURES

Pier Paolo Diotallevi[1], Luca Landi[1], Filippo Cardinetti[1]

[1] *DISTART, Department of Civil Engineering, University of Bologna, Italy*
Email: pierpaolo.diotallevi@mail.ing.unibo.it, luca.landi@mail.ing.unibo.it, filippo.cardinetti@unibo.it

ABSTRACT:

The object of this study is to develop an analytical model characterized by a mono-dimensional finite element able to reproduce the non-linear flexural-shear interaction of RC shear-critical structures. In the paper, the finite element formulation and the constitutive relationships that allow coupling between flexure and shear are illustrated together with a brief description of the algorithm which was implemented in an original computer program. The model was validated and calibrated by comparison with experimental results. Then, several numerical investigations were performed with the proposed model in order to study the effects of non-linear shear deformations for squat RC members.

KEYWORDS: RC Members, Non-linear Analysis, Fibre Beam-Column Model, Shear-Flexure Interaction.

1. INTRODUCTION

The non-linear behaviour of short RC structural elements has been studied, in general, according to different approaches, typically based on bi-dimensional finite elements. In some cases also mono-dimensional finite element extended for including the effects of shear has been used. The principal purpose of this research is to develop a fibre beam-column element which is able of describing the flexure-shear interaction and the shear response in the non-linear range. In the category of fibre elements at the date few models (Pietrangeli et al., 1999; Ceresa et al., 2006; Ceresa et al., 2007) have been proposed for describing the non-linear response of structures dominated by shear response, especially in the case of cyclic or dynamic loading. Most of proposed models for shear behaviour, as the "strut and tie" models, consider an uncoupled flexural and shear response. The models which can overcome this problem are usually based on biaxial constitutive laws. They are implemented in bi-dimensional finite elements which can not be easily used for the analysis of complex frame structures. Their implementation is rather limited to single structural elements or sub-assemblages. A theory that studies shear behaviour of RC elements is the Modified Compression Field Theory (MCFT) proposed by Vecchio and Collins (1986; 1988). In the study illustrated in the present paper a constitutive law based on this theory was introduced into a flexibility-based fibre element (Filippou et al., 1996). The element was extended in order to include non-linear shear deformations. In particular, the biaxial constitutive law was used for modelling the behaviour of each fibre. The element was implemented in a special purpose FEM program which is able to model generic frames. This computer program was also tested to check its working and its field of applicability. Then, a numerical study on the influence of the non-linear shear response was performed.

2. FIBRE ELEMENT FORMULATION

The fibre beam-column finite element, illustrated in Figure 1, is based on the model proposed by Filippou et al. (1991). The element generalized forces (Fig. 2) are grouped as shown in Eqn.2.1:

$$\mathbf{Q}=\begin{Bmatrix}Q_1\\Q_2\\Q_3\end{Bmatrix};\quad \mathbf{q}=\begin{Bmatrix}q_1\\q_2\\q_3\end{Bmatrix};\quad \mathbf{D}(x)=\begin{Bmatrix}M(x)\\T(x)\\N(x)\end{Bmatrix};\quad \mathbf{d}(x)=\begin{Bmatrix}\chi(x)\\\gamma(x)\\\varepsilon(x)\end{Bmatrix} \tag{2.1}$$

The vector **Q** represents the generalized nodal forces, **q** the generalized nodal displacements, **D**(x) the section internal actions and **d**(x) the section deformations. Deformations of the generic cross-section are characterized by the curvature χ, the axial strain ε at the centre and the shear strain γ. In the following Δ indicates the increment of all quantities for a step of analysis. In the two-field mixed method, independent shape functions are used for approximating the force and deformation fields:

$$\Delta\mathbf{d}^i(x)=\mathbf{a}(x)\cdot\Delta\mathbf{q}^i;\quad \Delta\mathbf{D}^i(x)=\mathbf{b}(x)\cdot\Delta\mathbf{Q}^i \tag{2.2}$$

In Eqn. 2.2 **a**(x) and **b**(x) are respectively interpolation matrices of deformations and forces while i indicates the iteration of structure state determination. Since interpolation functions are assumed dependent on flexibility, they are characterized by changing values during the analysis. A particular choice of the interpolation function **a**(x) allows some simplification:

$$\mathbf{a}(x)=\mathbf{f}^{i-1}\cdot\mathbf{b}(x)\cdot\left[\mathbf{F}^{i-1}\right]^{-1} \tag{2.3}$$

where $\mathbf{f}^{i-1}$ is the section flexibility matrix and $\mathbf{F}^{i-1}$ is the element flexibility matrix. These interpolation functions allows to correlate increment of nodal displacements $\Delta\mathbf{q}^i$ with increment of section deformations $\Delta\mathbf{d}^i$:

$$\Delta\mathbf{d}^i(x)=\mathbf{f}^{i-1}\cdot\mathbf{b}(x)\cdot\left[\mathbf{F}^{i-1}\right]^{-1}\cdot\Delta\mathbf{q}^i \tag{2.4}$$

With these interpolation functions the element equilibrium equation becomes:

$$\left[\mathbf{F}^{i-1}\right]\cdot\Delta\mathbf{q}^i=\mathbf{P}^i-\mathbf{Q}^{i-1} \tag{2.5}$$

where $\mathbf{P}-\mathbf{Q}^{i-1}$ are the applied unbalanced forces.

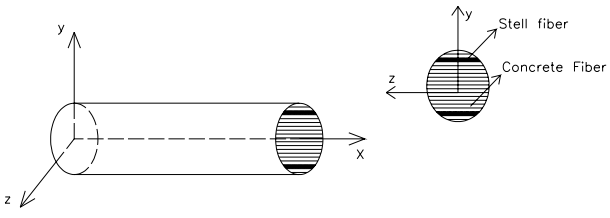

Figure 1 Fibre beam-column model

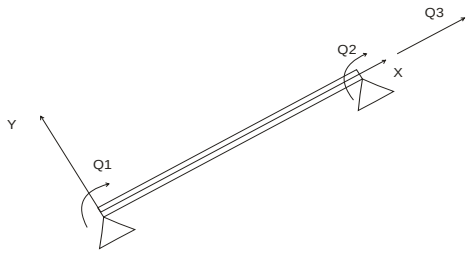

Figure 2 Finite element forces

3. MODIFIED COMPRESSION FIELD THEORY AS CONSTITUTIVE RELATIONSHIP

The Modified Compression Field Theory developed by Vecchio and Collins (1986) is characterized by a rotating smeared-crack model that represents concrete as an orthotropic material. All equations are formulated in terms of average stresses and strains. A local stress conditions at crack locations is however considered. Crack shear slips are not calculated and not accounted for in the element deformations. The further development of this theory is the Disturbed Stress Field Model (DSFM) which was proposed by Vecchio (2000; 2001) as an alternative formulation able to provide a better representation of concrete behaviour by including the relation between crack shear stress and crack shear slip.

3.1. Equilibrium condition

Let us consider a RC element (Fig. 3) subjected to uniform stresses $\boldsymbol{\sigma} = [\sigma_x \; \sigma_y \; \tau_{xy}]$.

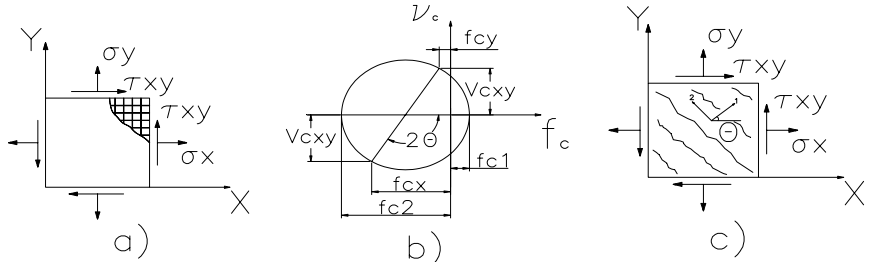

Figure 3 a), b) Element stresses, c) Principal stress directions

Equilibrium is examined on two levels: in terms of average stress smeared over the element area and of local condition along the crack surfaces. The principal stresses f_{c1} and f_{c2} are parallel and perpendicular to the crack direction defined by angle θ in Figure 3. The equilibrium equation for the reinforcements are:

$$\sigma_x = f_{cx} + \rho_x \cdot f_{sx}; \qquad \sigma_y = f_{cy} + \rho_y \cdot f_{sy}; \qquad \tau_{xy} = v_{cxy} \tag{3.1}$$

On crack surfaces the equilibrium condition is:

$$\sum_{i=1}^{n} \rho_i \cdot \left(f_{scri} - f_{si}\right) \cdot \cos^2 \theta_{ni} = f_{c1} \tag{3.2}$$

where ρ_i is the reinforcement ratio, f_{si} is the average stress in steel, f_{scri} is the local stress of the i-th reinforcement relating to ε_{scri} and the angle $\theta_{ni} = \theta - \alpha_i$, where α_i is the angle of reinforcement. The local increase of reinforcement stress, at crack location, leads to the development of shear stress v_{ci} along the crack surfaces:

$$v_{ci} = \sum_{i=1}^{n} \rho_i \cdot \left(f_{scri} - f_{si}\right) \cdot \cos\theta_{ni} \cdot \sin\theta_{ni} \tag{3.3}$$

3.2. Compatibility relationships

The continuum strain results from smearing of crack over a finite area, while the slip component results from rigid body movement along a crack interface. Total or "apparent" strains are denoted as $\boldsymbol{\varepsilon} = [\varepsilon_x \; \varepsilon_y \; \gamma_{xy}]$. The apparent inclination and principal strains can be calculated using Mohr circle. The shear slip and the associated deformation components are calculated as follows:

$$\gamma_s = \frac{\delta_s}{s}; \qquad \varepsilon_x^s = -\frac{\gamma_s}{2} \cdot \sin\left(2\theta\right); \qquad \varepsilon_y^s = \frac{\gamma_s}{2} \cdot \sin\left(2\theta\right); \qquad \gamma_{xy}^s = \gamma_s \cdot \cos\left(2\theta\right) \tag{3.4}$$

where δ_s is the slip along the crack surface and s is the crack spacing.

3.3. Constitutive laws

The principal compressive stress f_{c2} in the concrete is a function not only of the principal compressive strain, but also of coexisting principal tensile strain. The influence is captured by the reduction factor β_d, which is

calculated using expressions derived from experimental results. This factor is used to define both peak stress f_p and strain at peak stress ε_p:

$$f_p = -\beta_d \cdot f_c^{'}, \quad \varepsilon_p = -\beta_d \cdot \varepsilon_0 \tag{3.5}$$

The compression response curve of concrete is represented in Figure 4a while steel constitutive relationship is illustrated in Figure 4b. Slip δ_s is calculated according to two approaches (Vecchio, 2000): as a function of shear stress v_{ci} through a formulation which depends on crack width and compressive strength or as a function of angle of principal stress. The maximum of the two obtained values is considered.

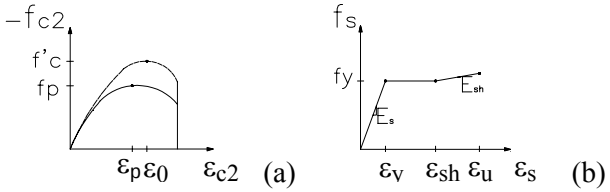

Figure 4 Consitutive laws for concrete (a) and steel (b)

4. IMPLEMENTATION OF THE MODEL

The model described so far was implemented in a special purpose program organized on three iteration levels. A Newton-Rapson (NR) iteration loop at structural level, an element state determination at element level (necessary for flexibility formulation) and another iteration loop at each fibre for application of Disturbed Stress Field Model (DSFM). The algorithm is organized in the following step:

1.Creation of initial stiffness structural matrix.
2.Application of load increment and NR iteration. Each NR iteration is indicated by a superscript *i*.
3.Calculation of nodal element displacements trough a condensation and a rotation matrix.
4.Beginning of element state determination procedure: calculation of nodal forces. Each iteration of element state determination is indicated by a superscript *j*.
5.Calculation of section forces in control sections.
6.Calculation of section deformations.
7.Calculation of fibre deformations.

8.Beginning DSFM at the fibre level. Each fibre is characterized by a deformation:

$$\boldsymbol{\varepsilon} = \left[\varepsilon_x \quad \varepsilon_y = 0 \quad \gamma_{xy} \right] \tag{4.1}$$

Initially it is assumed $\boldsymbol{\varepsilon} = \boldsymbol{\varepsilon}_c$. With application of Mohr circle principal strains $\boldsymbol{\varepsilon}_1$ and $\boldsymbol{\varepsilon}_2$ for concrete are obtained. The average strains ε_{sx} and ε_{sy} for steel are set equal to those of concrete along x and y axis. After calculating average stresses in concrete and steel through constitutive relations, local deformations in reinforcements ε_{sxcr} and ε_{sycr} on crack location are calculated through an iterative procedure:

$$\varepsilon_{sxcr} = \varepsilon_{sx} + \Delta\varepsilon_{1cr} \cdot \cos^2(\theta_\sigma); \qquad \varepsilon_{sycr} = \varepsilon_{sy} + \Delta\varepsilon_{1cr} \cdot \cos^2\left(\theta_\sigma - \frac{\pi}{2}\right) \tag{4.2}$$

At beginning of procedure $\Delta\varepsilon_{1cr} = 0$, then $\Delta\varepsilon_{1cr}$ is increased at each iteration until subsequent equilibrium equation is satisfied:

$$\rho_x \cdot \left(f_{sxcr} - f_{sx}\right) \cdot \cos^2\left(\theta_\sigma\right) + \rho_y \cdot \left(f_{sycr} - f_{sy}\right) \cdot \cos^2\left(\theta_\sigma - \frac{\pi}{2}\right) = f_{c1} \tag{4.3}$$

where stresses f_{sxcr} and f_{sycr} are functions of ε_{sxcr} and ε_{sycr} through constitutive relationship of steel. Then shear stress along crack surfaces are calculated:

$$v_{ci} = \rho_x \cdot \left(f_{sxcr} - f_{sx}\right) \cdot \cos\left(\theta_\sigma\right) \cdot \sin\left(\theta_\sigma\right) + \rho_y \cdot \left(f_{sycr} - f_{sy}\right) \cdot \cos\left(\theta_\sigma - \frac{\pi}{2}\right) \cdot \sin\left(\theta_\sigma - \frac{\pi}{2}\right) \tag{4.4}$$

where θ_σ is the angle of principal stresses. Being s_x and s_y crack spacings in x and y directions it is possible to determine the crack spacing s and the crack width w:

$$s = \frac{1}{\frac{\sin\theta_\sigma}{s_x} + \frac{\cos\theta_\sigma}{s_y}}; \qquad w = \varepsilon_{c1} \cdot s \tag{4.5}$$

Once the shear slip is calculated, it is possible to know the value of γ_s and the strain components due to shear slip $\boldsymbol{\varepsilon}_s$ (Eqn. 3.4). Then strain components $\boldsymbol{\varepsilon}_c = \boldsymbol{\varepsilon} - \boldsymbol{\varepsilon}_s$ are obtained. Considering the new values of $\boldsymbol{\varepsilon}_c$, an iterative procedure begins, that stops when the difference between subsequent values of $\boldsymbol{\varepsilon}_c$ are smaller than a fixed tolerance. Once the convergence is reached, values of tangent modulus for the two principal directions are calculated form equations of constitutive laws. These values are introduced into diagonal matrices referred to principal directions. Trough rotation matrix it is possible to pass from system of principal axes to original system. The stiffness matrices of each fibre are assembled in order to obtain the modulus matrices $\mathbf{E}_s$ and $\mathbf{E}_c$ of all fibres of the section, which become bandwidth when flexure-shear coupling begins. From these matrices the stiffness matrix of section is obtained.

9.Calculation of section resisting forces $\mathbf{D}^j_R(x)$.
10.Calculation of unbalanced section forces $\mathbf{D}^j_u(x) = \mathbf{D}^j(x) - \mathbf{D}^j_R(x)$.
11.Determination of section residual deformations.
12.Determination of residual nodal displacements and then check of the convergence by energy criterion. If convergence is reached $\mathbf{Q}^i$ is set equal to $\mathbf{Q}^j$ and $\mathbf{K}^i_{ele}$ to $\mathbf{K}^j_{ele}$. Then another element is examined. When convergence is reached for all elements the procedure continues from step 13. If convergence is not achieved j is incremented to j+1and a new element iteration begins.
13.Caculation of resisting nodal forces $\mathbf{F}^i_R$ and of stiffness matrix of structure.
14.Calculation of unbalanced nodal forces $\mathbf{F}^i_u = \mathbf{P} - \mathbf{F}^i_R$ then check of the convergence at structural level. If convergence is achieved the NR procedure is stopped and a new load increment is applied, otherwise i is set equal to i+1 and another NR iteration is performed.

5. NUMERICAL INVESTIGATIONS.

5.1. Comparison between numerical and experimental results

The comparison was carried out on a shear wall loaded by a force at the top. Considered experimental data are those of Vulcano and Bertero (1987). The comparison was performed between numerical results obtained with proposed model, experimental results and numerical results obtained by the three vertical line element (TVLE) proposed by Vulcano and Bertero. Geometric layout of tested wall is illustrated in Figure 5. The comparison between numerical and test results, shown in Figure 6 in terms of base shear-top displacement curve, allowed calibration and validation of model.

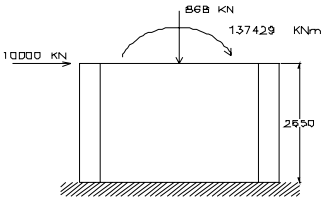

Figure 5 Tested wall

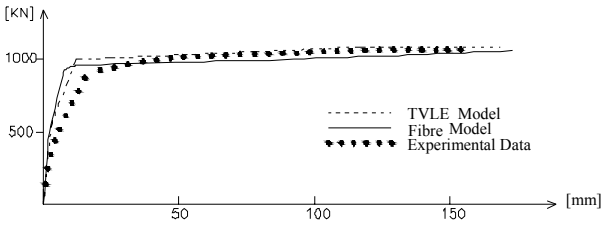

Figure 6 Comparison between numerical and experimental results

5.2. Analysis of a bridge pier

A bridge pier with circular cross-section loaded by a force at its free end was analyzed with the proposed model for investigating the non-linear flexure shear coupling. The analyses were repeated by changing the height of the pier L and by keeping the same section diameter D. Thus the control parameter of the analysis was the ratio L/D. Description of examined piers and of modelling assumptions are shown in Figures 7, Figure 8 and in Tab. 5.1. With regard to mechanical properties of materials, a concrete with cylinder compressive strength equal to 45 MPa and a steel with yielding stress equal to 430 MPa were considered. For each L/D ratio, two types of analysis were made: one considering non-linear flexural behaviour and linear shear response, uncoupled by the flexural one; the other considering coupled non-linear flexural and shear behaviour.

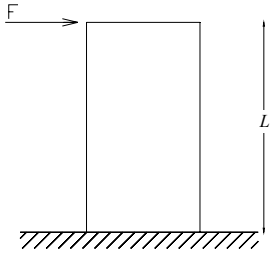

Figure 7 Pier under study

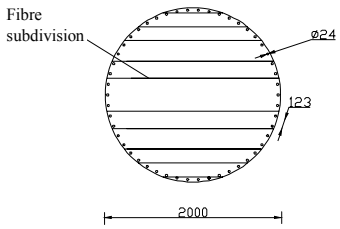

Figure 8 Fibre modelling of circular cross-secion

Tab. 5.1 Characteristics and modelling assumptions for considered RC piers

Diameter [m]	2	2	2	2	2	2	2	2	2	2
Height [m]	2	4	6	8	10	12	14	16	18	20
L/D	1	2	3	4	5	6	7	8	9	10
n. of elements	2	4	5	6	7	8	8	9	10	11
Element length	1.00	1.0	1.20	1.33	1.42	1.50	1.75	1.77	1.80	1.81

By calling with d_{MV} the top displacement associated to the base shear at yielding and calculated considering non-linear flexure-shear interaction, and with d_M the same type of displacement obtained by keeping linear the shear behaviour, the results of parametric analysis are illustrated in Figure 9a. In the Figure the ratio d_{MV}/d_M is plotted as a function of the ratio L/D. This graph shows that non-linear flexure-shear interaction affected the response in a significant way for values of L/D lower than 4. In Figure 9b V_M is the value of base shear calculated considering linear shear behaviour while V_{MV} is the value of base shear obtained considering non-linear shear behaviour. Figure 9b illustrates the ratio V_M/V_{MV} calculated at fixed values of top displacement in the non-linear range and plotted as a function of the ratio L/D. This diagram shows again the importance of non-linear shear response. Figure 10 illustratres the diagrams of base shear versus shear deformation evaluated at different locations along the height of the pier. This graph shows that the shear response did change along the height when non-linear flexure-shear interaction was included in the analysis. On the other hand the diagram of base shear versus shear deformation did remain linear and constant along the height when linear shear response was considered. Since shear forces are constant along the height while diagrams of shear versus shear deformation did change, it is clear that the variation of bending moment along the height did affect the shear deformations.

This result highlights the influence of flexure-shear interaction in the non-linear response.

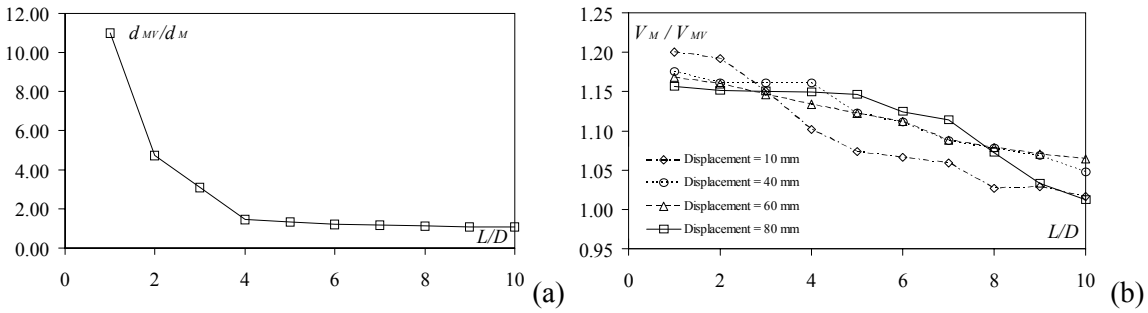

(a) (b)

Figure 9 Results of parametric analysis in terms of displacement (a) and base shear (b)

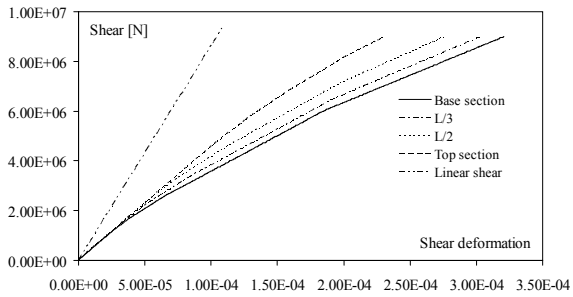

Figure 10 Diagrams of shear versus shear deformation for L/D =2

5.2. Analysis of a squat RC shear wall

The study is about a cantilever RC shear wall loaded by a force at its free end (Figure 11) and characterized by equal values of base length and height. With regard to mechanical properties of materials, a concrete with cylinder compressive strength equal to 30 MPa and a steel with yielding stress equal to 430 MPa were considered. In this analysis the wall was modelled with 2 elements and 3 control sections. From Figure 12, which shows the diagram of base shear versus top displacement and the diagram of base shear versus shear deformation, it is possible to observe that for this kind of wall the non-linear shear deformation was decisive.

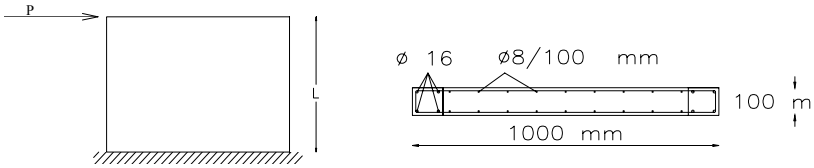

Figure 11 Geometry of the wall under study

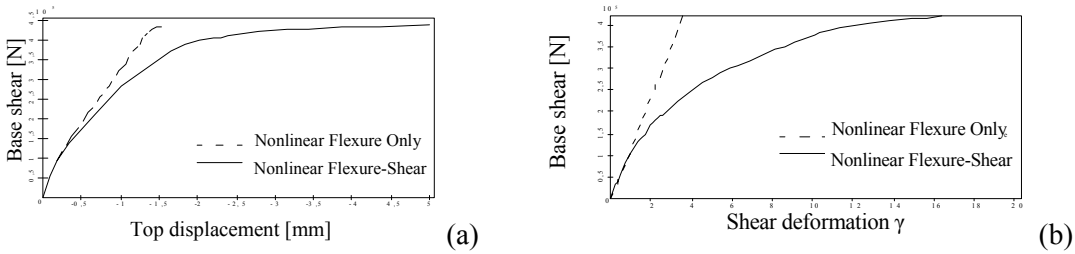

(a) (b)

Figure 12 Diagrams of base shear versus top displacement (a) and shear deformation (b)

Before cracking, the model based on non-linear shear deformations and the model based on elastic shear response produced same results. On the contrary the post-cracking structural behaviour was strongly influenced

by non-linear shear response (Fig. 12). Figure 13 represents the diagrams of stresses along the height of the fixed section. The stresses at the beginning of the analysis and the stresses after cracking are illustrated together in order to underline the modifications of stress distribution along the section height.

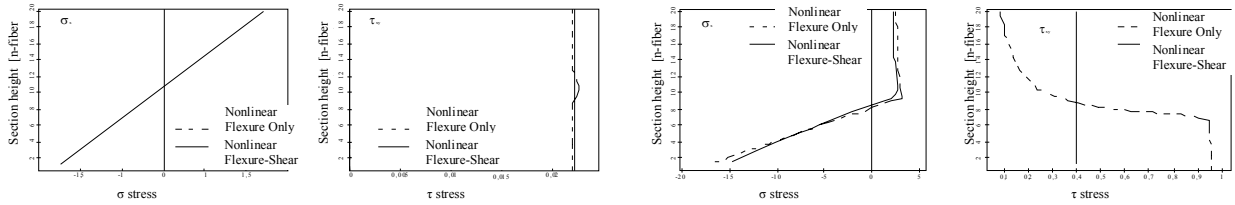

Figure 13 Stress distributions along the base section

6. CONCLUSIONS

A new fibre beam-column element able to reproduce the non-linear behaviour of squat structures was formulated and implemented in an original computer program. The main characteristics of the model are substantially the flexibility formulation and the constitutive relationship characterized by a rotating smeared-crack model. The proposed model was calibrated and validated through a comparison with experimental results and various numerical analyses were performed in order to study the influence of non-linear flexural-shear interaction. Analyses underlined that the model was able to reproduce flexure and shear non-linear response and above all, the coupling between flexure and shear in the non-linear range. This aspect did affect significantly the response of examined squat RC structural elements, especially in terms of deformation. This research is a starting point for further studies to improve and validate the model, for example through the comparison with cyclic loading test.

6. REFERENCES

Ceresa, P., Petrini, L. and Pinho, R. (2007). Flexure-shear fibre beam-column elements for modelling frame structures under seismic loading-state of the art. *Journal of Earthquake Engineering*, **11:1**.
Ceresa, P., Petrini, L., Pinho, R. and Auricchio, F. (2006). Development of a flexure-shear fibre beam-column element for modelling of frame structures under seismic loading. First European Conference on Earthquake Engineering and Seismology, Geneva, Switzerland, paper number 1425.
Filippou, F.C., Spacone, E. and Taucer, F.F. (1991). A fiber beam-column element for seismic response analysis of reinforced concrete structures. EERC Report no. 91/17, University of California, Berkeley.
Filippou, F.C., Spacone, E. and Taucer, F.F. (1996). A fiber beam-column model for nonlinear analysis of R/C frames: part.1 formulation. *Earthquake Engineering and Structural Dynamics*, **25**, 711-725.
Petrangeli, M., Pinto, P. and Ciampi, V. (1999). Fiber element for cyclic bending and shear of R/C structures. I: theory. *Journal of Engineering Mechanics*, **125:9**, 994-1001.
Vecchio, F.J. (2000). Disturbed stress field model of reinforced concrete: formulation. *Journal of Structural Engineering*, ASCE, **126:9**, 1070-1077.
Vecchio, F.J. (2001). Disturbed stress field model of reinforced concrete: implementation. *Journal of Structural Engineering*, ASCE, **127:1**, 12-20.
Vecchio, F.J. and Collins, M.P. (1986). The modified compression field theory for reinforced concrete element subjected to shear. *Journal of American Concrete Institute*, **83:2**, 219-231.
Vecchio, F.J. and Collins, M.P. (1988). Predicting the response of reinforced concrete beams subjected to shear using the modified compression field theory. *Aci Structural Journal*, **85**, 258-268.
Vulcano, A. and Bertero, V.V. (1987). Analytical models for predicting the lateral response of rc shear walls: evaluation of their reliability. Report EERC no. 87/19, University of California, Berkeley.